Mausam, (1996), **47**, 3, 237-250

551.553.21 : 551.515.1 : 551.43

Simulation of monsoon circulation and cyclones with different types of orography

ROY ABRAHAM K., S. K. DASH and U. C. MOHANTY
Indian Institute of Technology, New Delhi
(Received 25 November 1994, Modified 15 December 1995)

सार — ई. सी. एम. डब्ल्यू. एफ. स्पैक्ट्रल साधारण परिसंचरण निदर्श से पर्वतीय अभिलक्षण के विभिन्न प्रकारों पर कई सूक्ष्मग्राहिता प्रयोग इस अध्ययन में किए गए हैं। इसका मुख्य उद्देश्य विस्तृत पैमाने पर भारतीय ग्रीष्म कालीन मानसून के अभिलक्षणों का तथा चक्रवातों की गतिविधियों का अनुकरण करना है। पर्वतीय अभिलक्षण के मानों को प्रेक्षित मानों के निकटतम प्रस्तुत करने के लिए विभिन्न प्रकार के अंकीय फिल्टरों का उपयोग किया गया है। तुलनात्मक अध्ययन से ज्ञात होता है कि लैंकज़ोस फिल्टर सबसे अच्छे परिणाम देता है। अतः अनुवर्ती सुक्ष्मग्राहिता प्रयोगों में लैंकज़ोस फिल्टर का ही उपयोग किया गया है। बंगाल की खाड़ी में मानसून पूर्व ऋतु में मई के महीने में आए चक्रवात तथा मानसून के सबसे अधिकतम सक्रिय माह अगस्त में आए एक अन्य चक्रवात को संख्यात्मक प्रयोगों के लिए चुना गया है।

जब दो मानक विचलन आवरणीय पर्वतीय अभिलक्षणों का उपयोग किया गया तो मानसून वर्षा के अभिलक्षणों को विस्तृत पैमाने पर प्रेक्षित अभिलक्षणों के निकट पाया गया। निदर्श संयोजन के तीन दिन बाद, वर्षा वितरण में संयोजन की आरम्भिक अवस्थाओं की तुलना में सुधार हुआ। यद्यपि पूर्वानुमानित चक्रवात ने प्रेक्षित मार्ग का अनुसरण किया, परन्तु उसकी गति बहुत मंद थी। पर्वतीय अभिलक्षण के विस्तार के साथ प्रणालियां भी कुछ सुदृढ़ हुई हैं। पर्वतीय अभिलक्षणों में वृद्धि के साथ प्रणालियों की गतिविधियों में भी मामूली सी वृद्धि हुई है।

ABSTRACT. In this study a number of sensitivity experiments have been conducted with different types of orography in the ECMWF spectral General Circulation Model(GCM). The basic aim is to simulate the large scale features of the Indian summer monsoon and the movement of cyclones. Different types of digital filters have been used to represent the orography as close to the observed values as possible. A comparative study shows that the Lanczos filter gives the best results. Thus, the Lanczos filter has been used in subsequent sensitivity experiments. One cyclone over the Bay of Bengal during pre-monsoon month of May, and another during the most active month of August have been selected for numerical experiments.

The large scale features of the monsoonal rainfall were found to be close to those observed, when two standard deviation envelope orography was used. After 3 days of model integration, the rainfall distribution improved compared to the initial stages of integration. Although the predicted cyclone followed the observed track, the rate of movement was very sluggish. There was slight deepening of the systems with an increase of orography. The movement of the systems was also found to be slightly faster with the enhancement of orography.

Key words — Digital filters, Envelope orography, Gibbs' oscillation, Window functions, Spherical harmonics, Global Spectral Model, Simulation, Numerical experiments.

1. Introduction

It is well known that orography plays an important role in determining the characteristics of the summer monsoon, and the associated rainfall. Studies by Banerjee (1929), Das and Bedi (1978), Grossman and Durran (1984) show that the low level monsoon circulation is sensitive to the mountain barriers around that region. Studies also indicate the influence of orography on the formation, movement and the distribution of rainfall associated with a cyclone.

Hahn and Manabe (1975) used the General Circulation Model (GCM) of the Geophysical Fluid Dynamics Laboratory (GFDL) to study the effect of mountains, and carried out numerical experiments with and without mountain barriers. A comparison of model results with and without mountains shows how orography maintains an extended low pressure system at the right location.

The sensitivity experiments using the numerical models by Wallace *et al.* (1983), Jarraud *et al.* (1988) and Krishnamurti *et al.* (1984) show the importance of orography in the medium range (3-10 days) tropical forecasts and monsoon circulation. Experiments by Wallace *et al.* (1983) have shown that overall improvements in medium range tropical forecasts result from the use of envelope orography.

At all resolutions of triangular truncation, such as, T21, T42, T63 and T106, Jarraud *et al.* (1988) found that the impact of envelope causes a local modification, which tends to propagate and amplify (principally on synoptic scales) following the upper level flow. Using a global spectral model, Krishnamurti *et al.* (1984) showed that there is an improvement in the monsoon circulation over the region with the inclusion of envelope orography.

In this study numerical experiments have been conducted to examine the influence of different types of orography on large scale features of the monsoon and on the characteristics of cyclones. Section 2 deals with the Gibbs' oscillations associated with the representation of orography in spectral models. A brief description of the ECMWF model used in this study and the initial data preparation for different sensitivity experiments are given in Section 3 and 3.1, respectively. Section 3.2 gives a brief description of the use of digital filters to reduce the Gibbs' oscillations. Section 3.3 describes the synoptic features of the two cyclones selected as case studies. The general features of the monsoon and tropical cyclones simulated with the use of different orography and the Lanczos filter are discussed in Sections 4.1 and 4.2. Section 5 gives the conclusion of the study.

2. Use of orography in spectral models

The sigma and hybrid (Simmons and Burridge 1981) vertical descretization schemes require orography to be treated explicitly in the integration of the hydrostatic equation. The representation of orography in global spectral models is not straight forward. Usually U.S. Navy global orographic data, which are available at a resolution of 10 minutes, are interpolated to the transformed grid points of the model depending on its resolution. The orography thus obtained is rough and quasi-discontinuous resulting in the slow convergence of the spectral series of the dependent variables at the constant sigma/hybrid surfaces of the model and large truncation errors arise during numerical integration. Thus, there are problems of oceanic ripples, widening of continents and negative orography especially in the neighbourhood of narrow transition zones with steep slopes between mountain areas of plateau and the Gangetic plain. This affects the meteorological fields which are functions of surface geopotential heights. The quasi-discontinuity of the orography, such as, steep slopes results in the spurious Gibbs' oscillations whose amplitude decreases with increasing distance from such transition zones. This requires the orographic fields to be smoothed prior to their spherical harmonic representation. One such approach was suggested by Bourke *et al.* (1977) in grid point space. The smoothing can also be done by multiplying the original spectral amplitudes by certain window functions using nonrecursive digital filters. This approach suggested by Gorden and Stern (1974) has some advantages over the former. This method is simple to use and there is better control over the Gibbs' waves. The typical smoothing with a digital filter is done by using a 'low pass filter' which means that low frequencies are allowed to pass through and high frequencies are stopped with a transition zone between pass band and stop band.

The appropriate representation of orography still remains one of the major problems in model development. It is not known clearly which type of orography is best suited for a model. Different types of orography, such as, mean, envelope, silhouette, interpolated and significant height orography are used in GCMs. The enhancement in orography is done to represent the barrier effects of sub-grid scale ridges on the flow. Silhouette orography is the average of maximum heights in the profile of orography in the latitude and longitude directions over the model grid box. The model orography can also be obtained by interpolation of fine resolution data, such as, that of the U.S. Navy. The orography thus obtained is termed as interpolated orography.

3. Description of model

The T63 global spectral model of ECMWF at horizontal resolution T63 and with 19 hybrid levels in the vertical has been used for conducting sensitivity tests. The model is based on the spectral representation of non-linear coupled equations for momentum, thermodynamics, moisture, continuity and the hydrostatic relation. The basic prognostic variables of the model are vorticity, divergence, temperature, specific humidity and the logarithm of surface pressure. These prognostic quantities, the orography and the geopotential are represented in the horizontal by truncated series of spherical harmonics. All prognostic quantities and geopotential are carried on full index hybrid levels, whereas the vertical velocity is carried on half index level, subject to boundary conditions. In hybrid co-ordinate system, the upper level model surface "flattens" over steep terrains becoming

surfaces of constant pressure in the stratosphere and the lower level surface follows the earth's terrain. The conventional finite difference scheme in hybrid co-ordinate is used for vertical descretization.

For unaliased computation corresponding to T63 truncation, a transform grid with 96 Gaussian latitudes and 192 points along each longitude has been used in the model. For time integration, a semi-implicit scheme is used for equations of divergence, temperature and surface pressure. In this model, a linear fourth order diffusion is applied along the hybrid co-ordinate surfaces to avoid the spurious growth of amplitude at wave numbers near the truncation wave number.

The physics of the model corresponds to cycle 30 of ECMWF parameterization schemes. It includes: (*i*) the parameterization of planetary boundary layer, (*ii*) deep convection using Kuo's scheme, (*iii*) shallow convection, (*iv*) large scale precipitation, (*v*) the radiation scheme which takes into account the cloud-radiation interaction, (*vi*) partial cloud cover, (*vii*) multiple scattering and effect of gases and (*viii*) gravity wave drag. To adjust mass-wind imbalance, a diabatic version of normal mode initialization is used.

3.1. *Preparation of initial data set for experiments*

The initial data for the numerical experiments are prepared from the First GARP Global Experiment (FGGE) IIIB data set. The FGGE IIIB data are available on 1.875×1.875 degree latitude-longitude mesh over the entire globe on 15 levels. There are six multi-level fields at 10, 20, 30, 50, 70, 100, 150, 200, 250, 300, 400, 500, 700, 850 and 1000 hPa pressure levels. These fields are geopotential height in meters, zonal and meridional wind components in m/sec, temperature in degree Kelvin (°K), vertical velocity in hPa/sec and relative humidity (in %) below 300 hPa. Apart from these, FGGE data also contain mean sea level pressure.

The model needs the spectral components of atmospheric fields such as vorticity, divergence, temperature, logarithm of surface pressure and specific humidity consistent with the T63 truncation and surface fields, such as, orography, surface pressure, surface temperature, deep soil temperature, surface moisture, deep soil moisture, snow depth, land/sea mask, roughness length, solar albedo, climatic sea surface temperature and vegetation ratio at all the model grids (96×192) in the horizontal.

The meteorological fields are horizontally interpolated to 96×192 Gaussian grids (corresponding to T63 truncation) using the bicubic spline method. In the vertical, wind fields and temperature fields are interpolated to 19 level hybrid co-ordinates using log-log interpolation. Specific humidity is interpolated using linear interpolation because it is assumed to be varying linearly with height. The specific humidity is calculated from relative humidity and temperature with the help of a look-up table which gives the saturation vapour pressure corresponding to different temperatures. Using these interpolated fields in the grid space, input variables for the model, such as, vorticity, divergence, temperature and specific humidity for each hybrid level and also logarithm of surface pressure in spectral form are generated.

3.2. *Use of digital filters in orographic representation*

Orographic data (surface geopotential) for different sensitivity experiments are prepared by using the following expression,

$$\Phi_s = g(H_m + \alpha\sigma) \qquad (1)$$

where, g is accelertion due to gravity, H_m is the mean height (from the US Navy data set) on the Gaussian grids of the T63 model, α is the proportion of standard deviation to be added to the mean height over land points and σ is the standard deviation of mean height defined for the same grid as H_m. It may be noted that in the sensitivity experiments, the value of α used is made equal to zero (mean), 1, 1.5 and 2.

First of all the spectral fit is applied to the smoothed orography. The purpose of spectal fitting is to ensure consistency in T63 spectral resolution between the orographic field and the model resolution of upper air fields. Appropriate window functions are used to suppress orographic ripples as a consequence of spectral fitting. In this study, a digitally filtered field X has been expanded (Hogan and Rosmond 1991) in terms of spherical harmonics as:

$$\overline{X}(\lambda,\mu,\eta,t) = \sum_{m=-M}^{M} \sum_{n=|m|}^{N(m)} \sigma(n) X_n^m(\eta,t) P_n^m(\mu) \exp(im\lambda) \qquad (2)$$

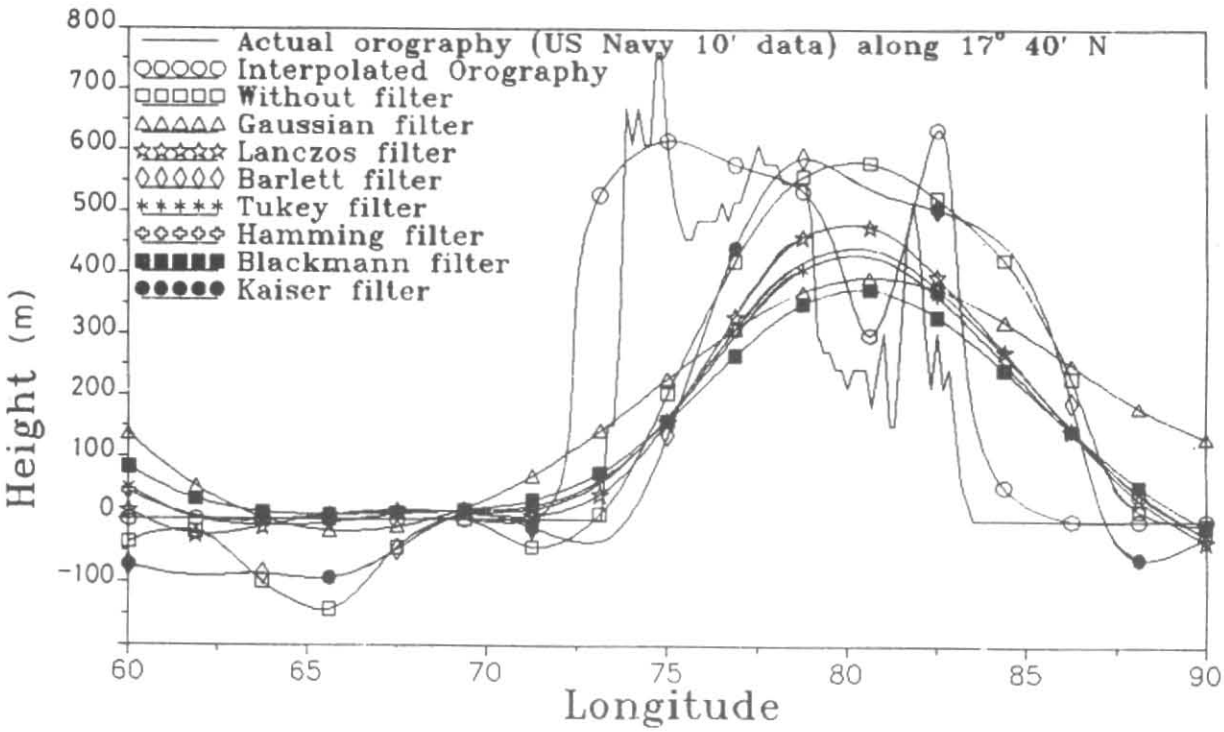

Fig. 1. Orography profile (m) along 17°40'N latitude smoothed with different filters in T63 model (cross section of Western Ghats)

Here, μ is the Sine of the latitude, λ is the longitude and P_n^m is the associated Legendre polynomial of the first kind with order m and degree n; m denotes planetary wave number and $(n\text{-}m)$ denotes the meridional wave number and η is the vertical hybrid coordinate. M and N are the largest Fourier wave number and the highest degree of Legendre polynomial for $m=0$ respectively. In the triangular truncation scheme used in this study, $N=M$.

Here, σ is termed as the 'window function'. Different types of digital filters can be defined depending on the functional behavior of $\sigma(n)$. Choice of 'window function' (Priestley 1981) will largely affect the representation of X in Eqn. (2). The important window functions used in this study are the rectangular window, Gaussian (Sardeshmukh 1984), Lanczos (1956), Tukey, Bartlett (Jenkins and Watts 1968), Hamming (1989), Blackmann (Johnson 1989) and Kaiser filter (Johnson 1989). Critical analysis of these filters is given in Stanley *et al.* (1984). In case of rectangular window, $\sigma(n)=1.0$ inside the truncation limit and zero otherwise. This amounts to no filtering in reality. In the frequency response, the width of the main lobe of the Bartlett filter is about twice as wide as that of the rectangular window. Gaussian filtering in spectral space is analogous to filtering by including diffusion terms in the physical space. Tukey window has significantly smaller side lobes which gives rise to less Gibbs oscillations. Hamming filter provides better control over transition band. Blackmann filter reduces the ripple height. Kaiser window provides better control over width of transition band and ripple height of Gibbs' oscillations, but it is computationally less efficient. The mathematical expression for the Lanczos filter used in Eqn. (2) in the model (Lanczos 1956) is given by:

$$\sigma(n) = \begin{cases} \left[\sin\frac{\pi n}{N}\right] \Big/ \left[\frac{\pi n}{N}\right], & |n| \leqslant N \\ 0, & |n| > N \end{cases} \qquad (3)$$

Thus, smoothing the partial sum by averaging over the period of the last term kept in the series results in Lanczos filter. The simplicity of the Lanczos filter makes it an attractive method of reducing Gibbs' oscillations. There is no definite criterion for the selection of best filter. The important criteria used in this study are the following:

(*i*) Maximum value of the filtered orography should be close to the actual highest orography.

(*ii*) Minimum value of filtered orography should be nearer zero.

(*iii*) Root Mean Square (RMS) error with reference to the actual orographic heights at model grids should be minimum.

Fig. 1 shows the cross section of filtered orography and US Navy orography along 17°40'N latitude over peninsular India. Fig. 3 shows the interpolated orography, unfiltered spectrally truncated orography (rectangular filter) and the orography smoothed by six digital filters over the peninsular India. Fig. 2 (a) shows the maximum height obtained from the interpolated orography, unfiltered spectrally truncated orography at horizontal resolutions T63, T106 and R45 and the digitally filtered orography at the same resolutions. Comparison shows that there is no clear superiority of any single filter over the rest in obtaining the maximum height and also the resolution has little role to play. The unfiltered orography as well as the Bartlett and Kaiser filters give the best value of maximum height followed by Lanczos filter. Other four filters give the lowest value of maximum height with very little difference. Similarly Fig. 2 (b) gives the minimum (or maximum negative) value of orography which is obviously zero in case of the interpolated orography. Comparison shows that unfiltered orography, Bartlett and Kaiser filters give the maximum negative values and the triangular truncation gives definitely better results than the rhomboidal truncation for the same degrees of freedom (T63 and R45). However, T106 resolution does not show any significant improvement over T63. As discussed earlier, the maximum heights obtained [Fig. 2 (a)] in case of Bartlett and Kaiser filters are close to the interpolated value. However, because of the maximum negative values (ripples), the Bartlett and Kaiser filters are as worse as unfiltered orography so far as Gibbs' oscillations are concerned. Gaussian filter gives the least negative orography [Fig. 2 (b)]. All other filters including Lanczos give moderate negative orography. Fig. 2 (c) shows the RMS errors with reference to the interpolated orography. Gaussian filter gives the maximum error, even more than the unfiltered values. Hence, Gaussian filter is not selected inspite of its giving the least ripples [Fig. 2 (b)]. Lanczos filter gives RMS error close to those obtained in case of Bartlett and Kaiser filters, which are the least RMS errors. Considering the combined effect of all the three aspects such as the maximum height, negative orography and the RMS error, Lanczos filter seems to perform reasonably well. Hence, Lanczos filter will be used to reduce the Gibbs' oscillations in the representation of orography in the GCM at resolution T63 for conducting sensitivity tests.

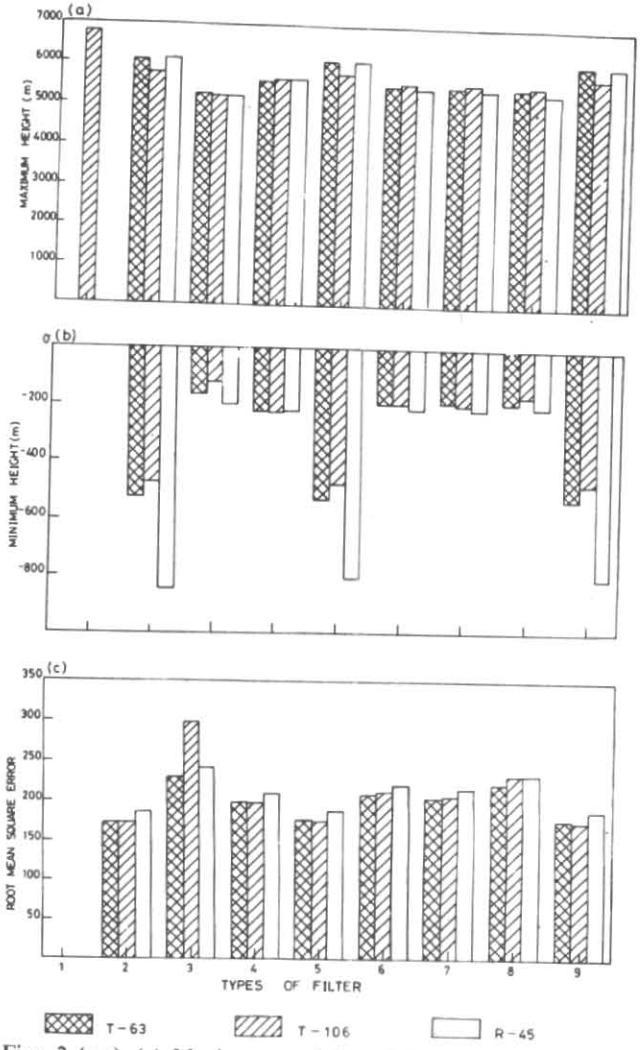

Figs. 2 (a-c). (a) Maximum and (b) minimum height (m) of orography and (c) root mean square error obtained with various filters at different model resolutions. The number (1) along the x-axis stands for the interpolated orography and subsequent numbers stand for the filters, (2) Rectangular, (3) Gaussian, (4) Lanczos, (5) Berlett, (6) Tukey, (7) Hamming, (8) Blackmann and (9) Kaiser

3.3. *Synoptic description of cyclones and design of experiments*

The tropical cyclone over Bay of Bengal during 8-16 May in the pre-monsoon phase and other during 6-14 August representing the active phase of monsoon have been selected for the simulation of the model. The cyclone of May 1979 was formed at an unusually low latitude (6.5°N) and had a long life of 8 days (Mukherjee *et al.* 1981). This cyclone had its genesis as a low over southeast Bay of

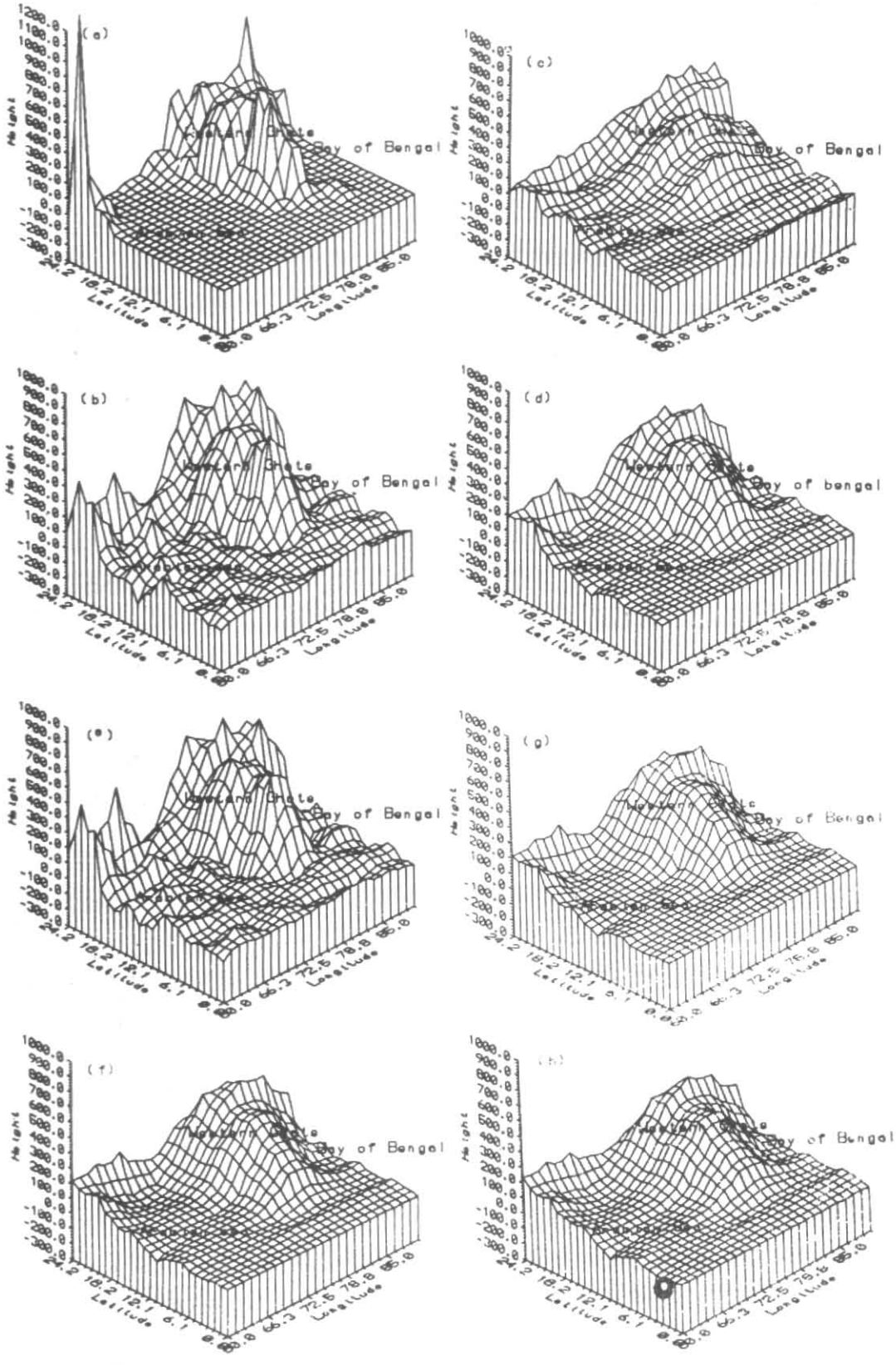

Figs. 3 (a-h). Surface profile of orography (m) over peninsular India smoothed with different filters in T63 model (a) Inter polated orography, (b) Rectangular filter, (c) Gaussian filter, (d) Lanczos filter, (e) Tukey filter, (f) Hamming filter. (g) Blackmann filter and (h) Kaiser filter

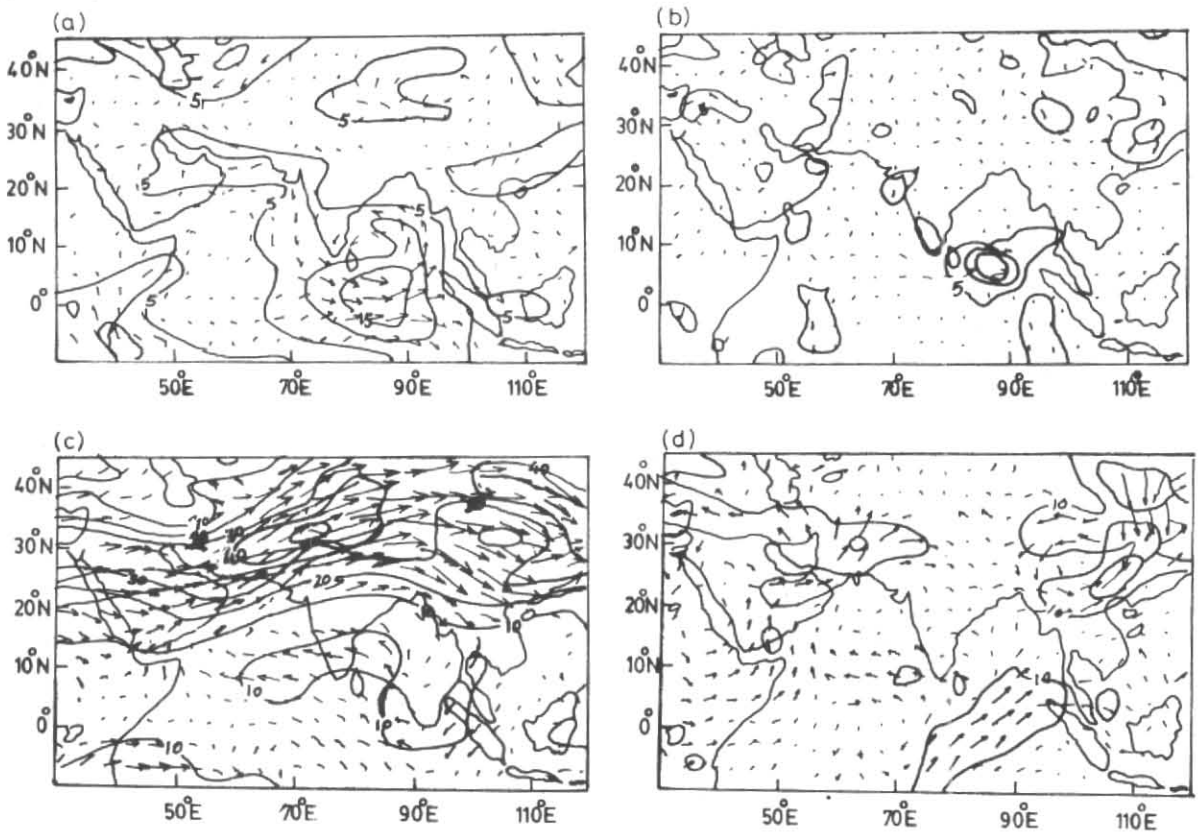

Figs. 4 (a-d). Vector wind and isotachs at (a & b) 850 hPa and (c & d) 200 hPa when model was integrated from 8 May 1979 with mean orography : (a) day one prediction & (b) prediction minus analysis at contour interval 5 m/s and with two standard deviation envelope orography : (c) day three prediction & (d) prediction minus analysis at contour interval 10 m/s

Bengal, which slowly intensified into a depression on 5 May with its centre near 7°N, 88°E. The storm took a west-southwesterly track up to 8th morning and formed a cyclonic loop near 6°N, 86°E. Satellite Tropical Disturbance Summary (STDS) from Washington classified this system as T4.5 on Dvorak's scale on 8th, which corresponds to a maximum wind of 39.6 m/sec.

Under the influence of a low pressure wave moving westwards across the Arakan coast, a low formed over the north Bay of Bengal on 5 August. It intensified into a deep depression on the morning of 6th with its centre near 21°N, 90°E. Moving slowly in a westward direction, and progressively intensifying, it became a cyclonic storm by the 7th morning. It developed into a severe cyclonic storm on the same afternoon. Since the storm was covered by general monsoon cloudiness, it could not be classified according to Dvorak's scale based on satellite pictures.

In the first set of sensitivity experiments, the model has been integrated for 10 days starting from the initial date of 8 May, 1979. Four cases of sensitivity studies have been conducted with mean orography and with envelope orography of $\alpha = 1$, 1.5 and 2. In the second set of experiments, the model has been integrated for 10 days starting from the initial date of 6 August, 1979. Three experiments have been conducted using mean orography and envelope orography with $\alpha = 1$ and 2. Lanczos filter was used for smoothing the orography for these experiments. Important meteorological parameters such as wind and geopotential height at different levels of the model, the mean sea level pressure and the accumulated rainfall obtained after each day of integration, with mean and enhanced orography have been analyzed. However, to save space, only selected figures corresponding to envelope orography of $\alpha = 2$ are shown.

4. Results and discussion

4.1. *Results of 8 May 1979 cyclone simulation*

The predicted wind field after 24 hours of model integration with mean orography and the difference between the prediction and corresponding ECMWF analysis have been shown in Figs. 4 (a & b). As seen

TABLE 1

Some features of the simulated cyclone of 8 May 1979

Parameters	Mean orography			2σ envelope orography			ECMWF analysis/observed		
	day 1	day 3	day 5	day 1	day 3	day 5	9 May	11 May	13 May
Centre of the cyclone at 850 hPa (± 1° lat/long)	82°E 10°N	82°E 12°N	80°E 13°N	82°E 10°N	82°E 12°N	79°E 14°N	81°E 11°N	79°E 13°N	78°E 16°N
Geopotential height at 850 hPa (± 20 gpm)	1440	1430	1400	1440	1430	1400	1420	1430	1430
MSL pressure (± 2 hPa)	1000	1000	996	1000	996	992	998	996	998
Maximum rainfall (± 10 mm/day)	30	20	50	30	30	50	55	20	64

in Fig. 4 (b) there is not any significant difference between the day 1 prediction and analysis over the Indian landmass. However, large anomaly is observed mainly to the south of the observed cyclone centre. This may be due to inadequate data coverage over the cyclonic region and also due the fact that the centre of the predicted cyclone is not at the same location as the observed one. The approximate positions of the centre of the cyclone based on the ECMWF analysis and predicted by the model with different types of orography are given in Table 1. Comparison shows that use of mean orography or envelope orography gives the same position of the centre of the cyclone on days 1 and 3 of prediction. However, on day 5, the two standard deviation envelope orography simulates the centre of the cyclone closer to the position in the corresponding analysis compared to that with mean orography. Comparing the positions of predicted cyclone after day 1 and day 5 it is found that the cyclone has moved to the north by about 3° latitude in case of mean orography and by 4° in case of two standard deviation orography. ECMWF analysis shows the movement of the cyclone by 5° to the north during the same period. Similarly, no significant difference in the distribution of predicted wind intensity over India is found when mean orography and envelope orography with $\alpha = 1$, 1.5 and 2 were used in the model. Figs. 4 (c & d) show, the anomaly and the wind fields after 72 hours of integration at 200 hPa when envelope orography with $\alpha = 2$ has been used in the model. A slight increase in wind strength is found around the cyclonic circulation [Fig. 4 (d)] with an increase of orography.

The predicted geopotential heights at 850 hPa after days 1, 3 and 5 and based on the ECMWF analysis are given in Table 1. Comparison shows that the geopotential heights simulated with mean and envelope orography are same up to day 5. The 24-hour predicted geopotential at 850 hPa is higher than the corresponding analysed value, whereas the predicted geopotential and the analysed value, are same on day 3. On day 5, the predicted geopotential is less than that in the analysis indicating that beyond 72 hours, a slight deepening of the cyclone is evident in the prediction.

In 24-hour prediction of MSL pressure (figure not shown), the minimum pressure increased from 998 to 1000 hPa over central India. A lateral spread of the minimum pressure over central India and the cyclonic region was observed with an increase of orography. The anomalies showed higher values over Srilanka and north India in case of enhanced orography. After 72 hours, the cyclonic system further deepened with a difference of 4 hPa (Table 1) between mean and envelope orography. Comparison with ECMWF analysis (Table 1) indicates that up to day 3, the predicted MSL pressure is either more or equal to that in the analysis, but the predicted cyclone deepened after that and the deepening is more in case of two standard deviation envelope orography. Figs. 5 (a-d) show the MSL pressure after 120 hours of model integration and the anomaly fields with mean and envelope orography respectively. Landfall occurred after 7 days and there was considerable filling up of the system.

The 24-hour accumulated rainfall obtained from the model simulation has been compared with daily

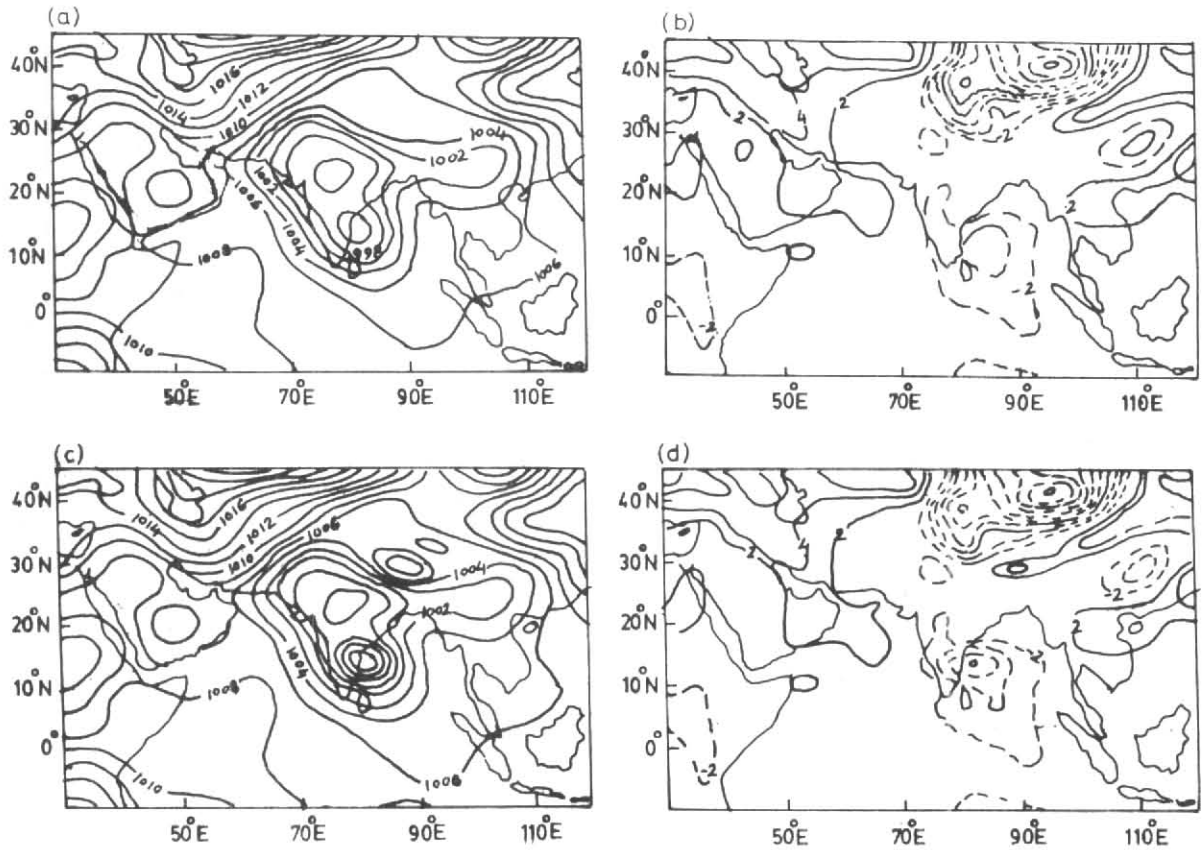

Figs. 5 (a-d). Mean sea level pressure when model was integrated from 8 May 1979 with (a & b) mean orography and (c & d) two standard deviation envelope orography: (a & c) day five prediction and (b & d) prediction minus analysis. Contour interval = 2 hPa

rainfall rates obtained from Krishnamurti *et al.* (1983). The latter rainfall was calculated from a combination of raingauge observation and satellite observations accumulated over 24 hours starting from 0000 hrs. The daily rainfall predicted in the present study is the 24-hour accumulated rain starting from 1200 hrs everyday. Rainfall after days 1, 3, 5 and 7 of model integration are shown in Figs. 6 (a-h) for mean orography and two standard deviation envelope orography. The values of maximum rainfall from prediction and observation are summarized in Table 1. No noticeable difference in rainfall is observed when the mean [Fig. 6 (a)] and envelope orography with $\alpha = 2$ [Fig. 6 (b)] are used in the model in the first 24 hours of integration. The predicted center of maximum rainfall is found to be to the south of the observed center of maximum rainfall by about 5° latitude. The maximum observed rainfall is of the order of 55 mm with wide-spread rainfall over the oceanic region. After 72 hours an increase of about 10 mm of rainfall is observed in the northeast quadrant of the tropical cyclone with envelope orography [Fig. 6 (d)] compared to the mean orography [Fig. 6 (c)]. On 11 May, the observed rainfall shows a decrease from 50 to 20 mm compared to the rainfall on 9 May. However, the predicted rainfall with two standard deviation envelope orography [Fig. 6 (d)] gives an overestimate of 10 mm over the storm region. Widespread rain over south India especially off the coast of Kerala and northern Bay of Bengal is found after 5 days of integration (Figs. 6 (e & f)]. However, the rainfall amount is less than that observed (Table 1).

After 7 days, the predicted rainfall distribution shows little northward progress of the cyclone (Fig. 6 (g)]. The observed rainfall maximum on 15 May is found to be in the Gangetic plain with a value of 67 mm. The predicted rainfall due to envelope orography with $\alpha = 2$ gives higher rainfall over the north Bay of Bengal and the coastal Kerala after 5 days [Fig. 6 (h)] of model integration compared to that with mean orography [Fig. 6 (g)]. Eventhough predicted rainfall is highly underestimated with respect to the observed rainfall in the initial 24 hours of

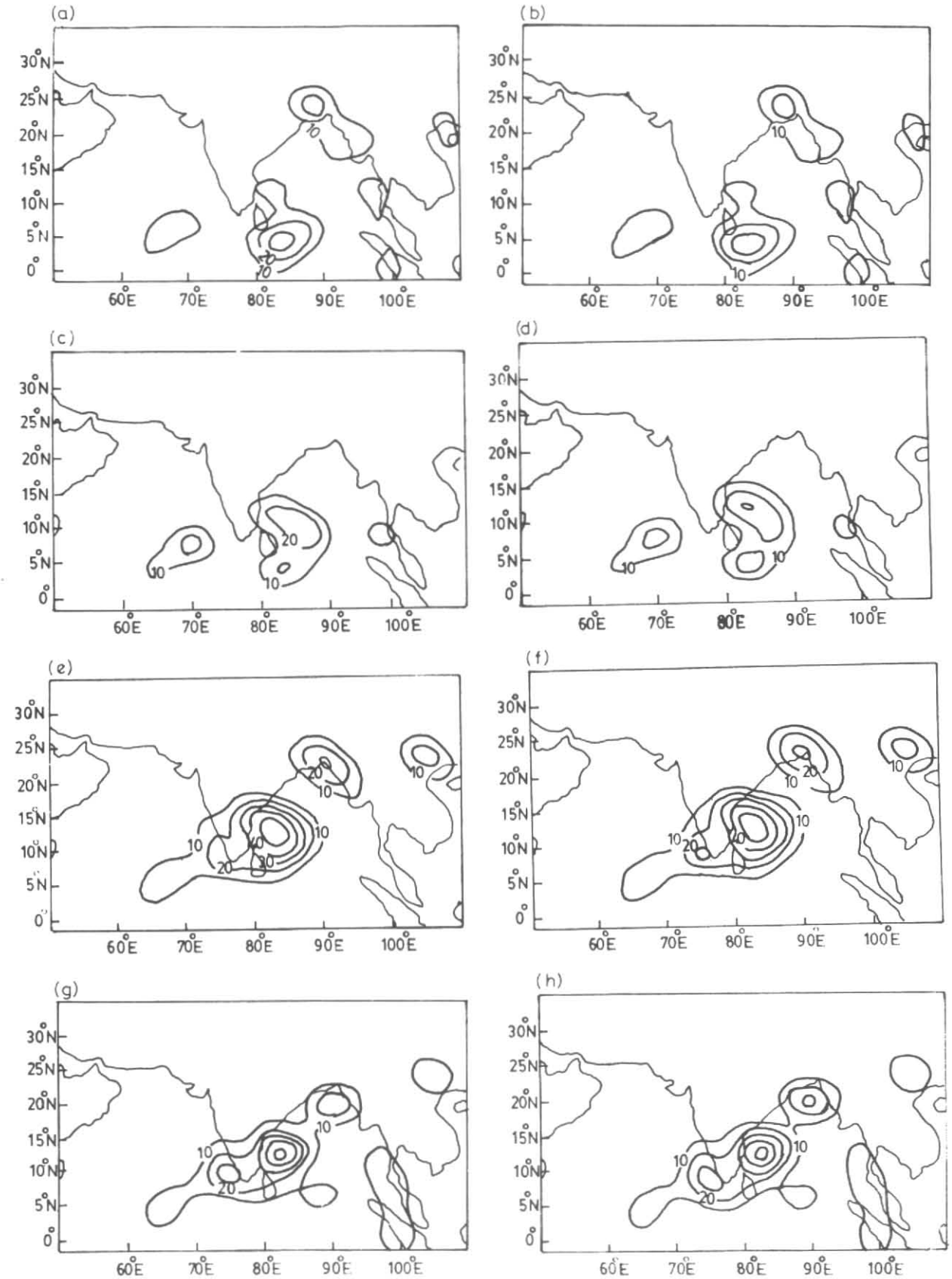

Figs. 6 (a-h). 24-hour accumulated rainfall after (a & b) one day. (c & d) 3 days. (e & f) 5 days and (g & h) 7 days integration of model from 8 May 1979 (a. c. e & g) with mean orography (b, d, f & h) with two standard deviation envelope orography. Contour interval = 10 mm/day

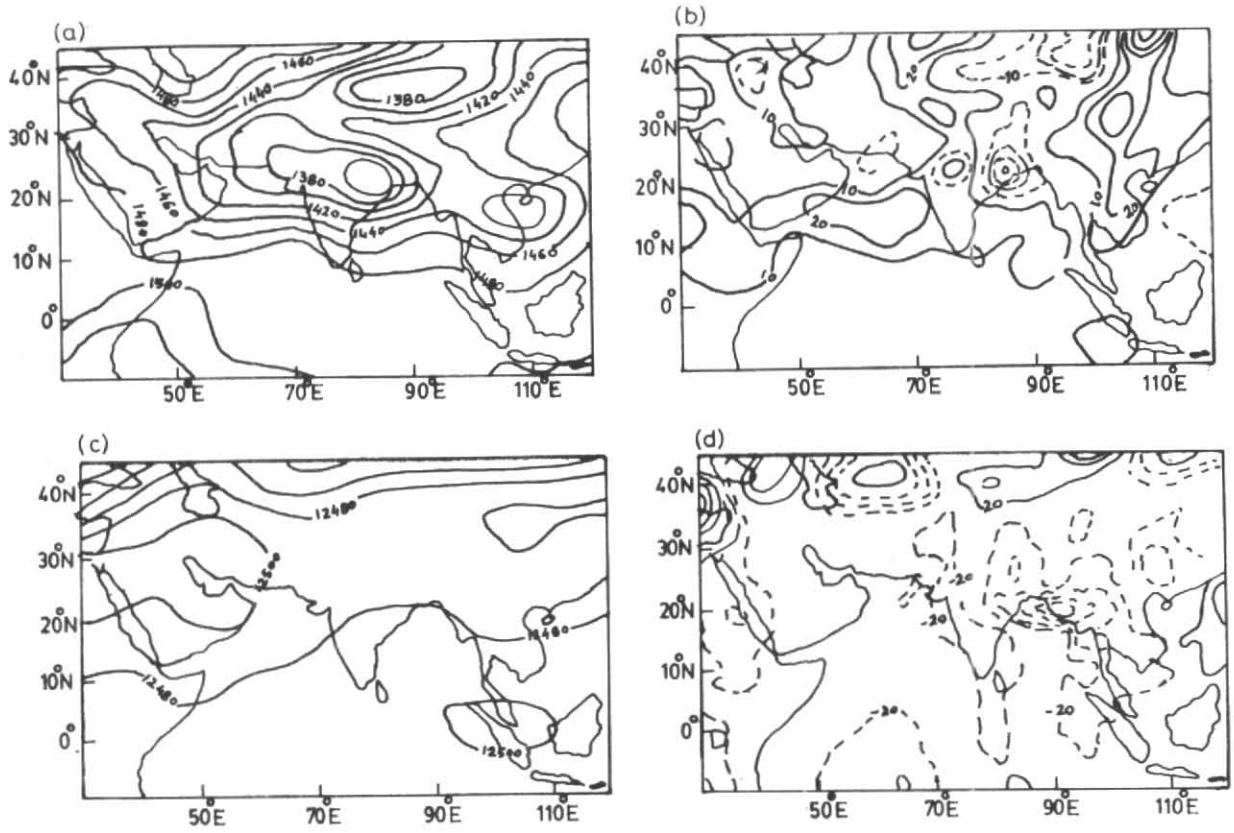

Figs. 7 (a-d). Geopotential at (a & b) 850 hPa and (c & d) 200 hPa when model was integrated from 6 August 1979 with mean orography (a & c) day three prediction and (b & d) prediction minus analysis. Contour interval = 20 m

integration, improvement is observed with the use of envelope orography with $\alpha = 2$.

4.2. *Results of 6 August cyclone simulation*

The T63 model was also integrated from 6 August 1979 for 10 days with mean and envelope orography. The results of the sensitivity experiment starting from 6 August 1979 are briefly discussed below. The results, at large, indicate the same characteristics of the role of envelope orography as obtained in case of 6 May cyclone. The predicted geopotential heights at 850 and 200 hPa after 72 hours with mean orography are shown in Figs. 7 (a) & (c) respectively. The difference fields from the respective analysis are shown in Figs. 7 (b) & (d) respectively. With the enhancement of orography upto $\alpha = 2$, no significant difference is found (figures not shown) in the geopotential field at 850 and 200 hPa. After 120 hours of integration, little difference is obtained in the geopotential with different orographies, except at the 200 hPa level.

The minimum value of predicted MSL pressure is found to be 988 hPa with mean orography [Fig. 8 (a)] and envelope orography (figure not shown) after 24 hours of integration. However, the system is found to have weakened after 72 hours with the minimum pressure increased to 990 hPa [Fig. 8 (c)]. The very slow movement of the cyclone delayed the landfall. The anomaly in case of envelope orography [Fig. 8 (d)] with $\alpha = 2$ is less than that with the mean orography (Fig. 8 (b)] by 2 hPa. Though the system was observed to move westwards, subsequent integrations of the model indicate its southwestward movement. The MSL pressure is found to have decreased to 986 hPa after 5 days of integration with envelope orography with $\alpha = 2$.

In the first 24-hour model integration, the mean orography [Fig. 9 (a)] and envelope orography [Fig. 9 (b)] with $\alpha = 2$ give more than 20 mm of rainfall off the west coast of peninsular India. After 3 days, due to the intensification of Somali current, 20 mm rainfall is observed off the coast of Somalia [Figs. 9 (c & d)]. After 5 days of model integration, the mean orography gives a maximum rainfall of 30 mm [Fig. 9 (e)] off the western coast of peninsular India while the

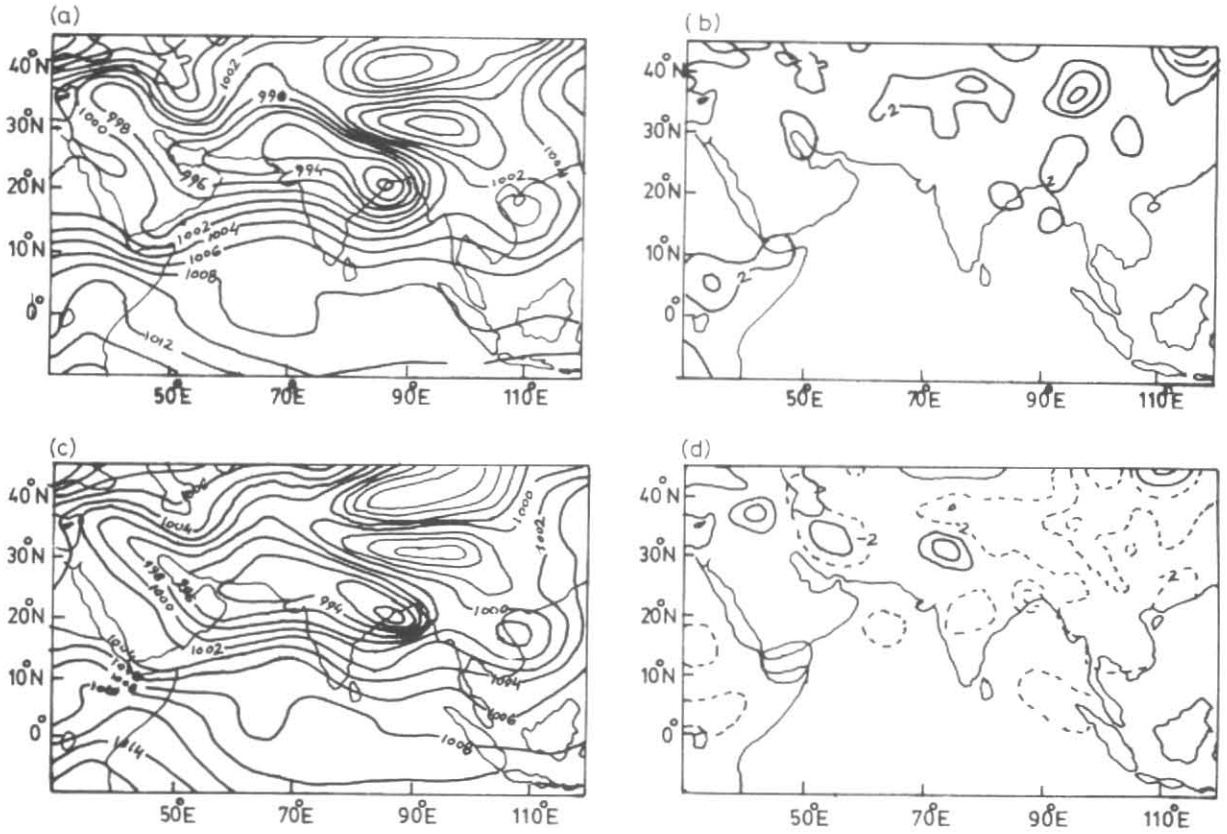

Figs. 8 (a-d). Mean sea level pressure when model was integrated from 6 August 1979 with mean orography : (a) day one prediction & (b) prediction minus analysis and with two standard deviation envelope orography : (c) day three prediction & (d) prediction minus analysis. Contour interval = 2 hPa

envelope orography gives 20 mm [Fig. 9 (f)] rainfall. On the other hand, the maximum rainfall over cyclone region shows 50 mm for the mean orography and 60 mm for the envelope orography with $\alpha = 2$ [Figs. 9 (e & f)]. The subsequent integrations do not show any substantial difference.

5. Conclusions

With the introduction of envelope orography, the geopotential shows higher value after 3 days of prediction at 200 hPa pressure level. The geopotential at 850 hPa is not affected by different types of orography. The MSL pressure and the rainfall both show higher values after 3 days of prediction when envelope orography is introduced in the model. In general, the results indicate an improvement in the prediction of the large scale features of monsoon circulation and rainfall with two standard deviation envelope orography compared to the mean orography.

No distinguishable feature was observed on the landfall of cyclones. Though the cyclones in general followed the observed tracks, the movement of both is found to be sluggish. The movement of both the systems is found to be slightly faster with the increase of orography. Though the predicted MSL pressure pattern over the cyclone region is weaker than the observed value, the system in general is reasonably well simulated. A slight deepening of the system is observed with two standard deviation envelope orography. The sudden weakening of the cyclone can also be noticed with the land fall. The model-predicted rainfall rates are found to be spread over very large area. After 3 days of integration, the rainfall patterns show better agreement with the observations compared to the initial stages of integration especially with two standard deviation envelope orography.

Acknowledgement

The authors acknowledge the support provided by the NCMRWF, New Delhi for carrying out the sensitivity experiments on the CRAY supercomputer.

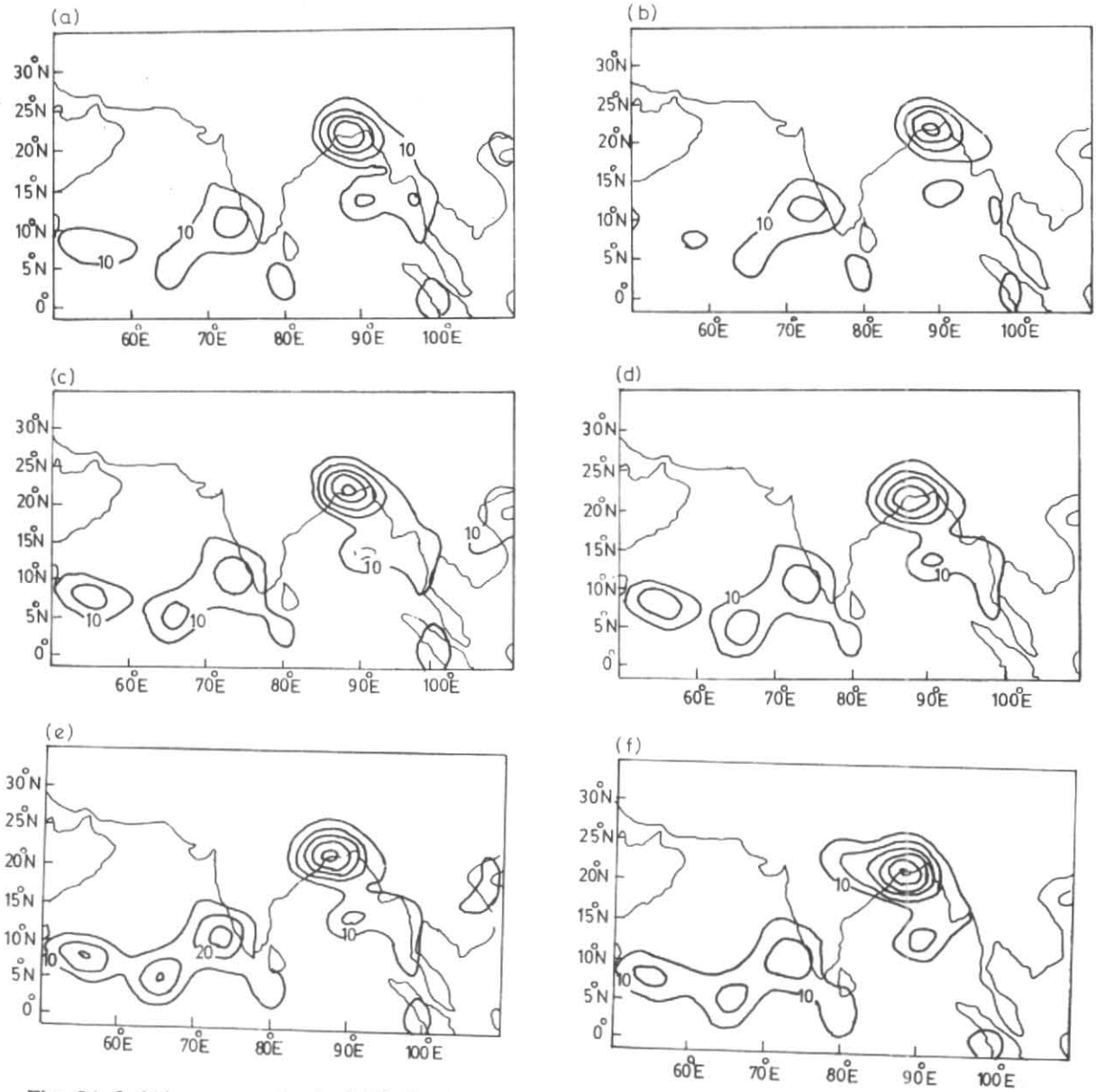

Figs. 9 (a-f). 24-hour accumulated rainfall after (a & b) one day, (c & d) 3 days and (e & f) 5 days of model integration from 6 August 1979 (a, c & e) with mean orography & (b, D & f) with two standard deviation envelope orography. Contour interval = 10 mm/day

References

Banerjee, S. K., 1929, "The effect of the Indian mountain ranges on the configuration of the isobars", *Indian J. Phys.*, IV, 477-502.

Bourke, W. B., McAvaney, B., Puri, K. and Thruling, 1977, "Global modelling of atmospheric flow by spectral methods", Methods in the Computational Physics, **17**, ed. J. Chang, Academic Press, 267-324.

Das, P. K. and Bedi, H. S., 1978, "The inclusion of Himalayas in a primitive equation model", *Indian J. Met. Hydrol. Geophys*, **29**, 373-383.

Gordon, T. and Stern, W., 1974, "Spectral modelling at GFDL", GARP WGNE Report No. 7, 46-82.

Grossman, R. L. and Durran, D. R., 1984, "Interaction of low-level flow with the Western Ghat mountains and off shore convection in the summer monsoon", *Mon. Weath. Rev.*, **112**, 652-671.

Hahn, D. G. and Manabe, S., 1975, "The role of mountains in the south Asia monsoon circulation", *J. Atmos. Sci.*, **32**, 1515-1541.

Hamming, R. W., 1989, "Digital filters", Prentice-Hall International, 284 p.

Hogan, T. F. and Rosmond, T. E., 1991, "The description of the Navy operational Global Atmospheric prediction systems spectral forecast model", *Mon. Weath. Rev.*, **119**, 1786-1815.

Jarraud, M., Simmons, A. J. and Kanamitsu, M., 1988, "Sensitivity of medium-range weather forecasts to the use of an envelope orography", *Quart. J. R. Met. Soc.*, **114**, 989-1025.

Jenkins, G. M., and Watts, D. G., 1968, "Spectral analysis and its applications", Holden-Day, 525 p.

Johnson, J. R., 1989, "Introduction to digital signal processing", Prentice-Hall International, 40 p.

Krishnamurti, T. N., Cocke, S., Pasch, R. and Low-Nam, S., 1983, "Precipitation estimates from rain gauge and satellite observations-summer monex", FSU Report No. 83-7, May 1983, Department of meteorology, Florida State University, Tallahassee, Florida, 373 p.

Krishnamurti, T. N., Ingles, K., Cocke, S., Kitade, T. and Pasch, R., 1984, "Details of low latitude medium range numerical weather prediction using a global spectral model, Part II : effects of orography and physical initialization", *J. Meteor. Soc., Japan*, 613-648.

Lanczos, C., 1956, "Applied analysis", Prentice-Hall, 539 p.

Mukherjee, A. K., Ramakrishnan, A. R. and Jambunathan, R., 1981, "Cyclones and depressions over the Indian seas in 1979", *Mausam*, **32**, 115-126.

Priestley, M. B., 1981, "Spectral analysis and Time series", **Vol. 1**, Academic Press, pp. 561-566.

Sardeshmukh, P. D. and Hoskins, B. J., 1984, "Spatial smoothing on the sphere", *Mon. Weath. Rev.*, **112**, 2524-2529.

Simmons, A. J. and Burridge, D. M., 1981, "An energy and angular momentum conserving vertical finite difference scheme and hybrid vertical coordinates", *Mon. Weath. Rev.*, **109**, 758-766.

Stanley, W. D., Dougherty, G. R. and Dougherty, R., 1984, "Digital signal processing", Reston, 514 p.

Wallace, J. M., Tibaldi, S. and Simmons, A. J., 1983, "Reduction of systematic forecast errors in the ECMWF model through the introduction of an envelope orography", *Quart. J. R. Met. Soc.*, **109**, 683-718.